

Knudsen Layer Reduction of Fusion Reactivity

Kim Molvig, Nelson M. Hoffman, B. J. Albright, Eric M. Nelson, and Robert B. Webster
Los Alamos National Laboratory, MS B259, P.O. Box 1663, Los Alamos, New Mexico 87545, USA
(Received 5 April 2012; published 30 August 2012)

Knudsen layer losses of tail fuel ions can significantly reduce the fusion reactivity of multi-keV DT in capsules with small fuel ρr ; sizable yield reduction can result for small inertial confinement fusion (ICF) capsules. This effect is most pronounced when the distance from a burning DT gas region to a nonreacting or cold wall is comparable to the mean free path of reacting fuel ions. A simplified asymptotic theory of Knudsen layer tail depletion is presented and a nonlocal reduced fusion reactivity model is obtained. Application of the model in simulations of ICF capsule implosion experiments gives calculated yields and ion temperatures that are in much closer agreement with observations than are the results of “nominal” or mixed simulations omitting the model.

DOI: [10.1103/PhysRevLett.109.095001](https://doi.org/10.1103/PhysRevLett.109.095001)

PACS numbers: 28.52.Cx, 47.45.-n, 52.40.Hf, 52.57.-z

In a fusion plasma the ions responsible for the majority of fusion reactions have energies significantly higher than the average energy of the thermal ions. As a result, their mean free paths are much longer than those of the average thermal ions owing to the rapid decrease of the Coulomb collision cross section with energy, $\sigma_{\text{Coul}} \propto 1/E^2$. In a plasma near a boundary with a cold, nonreacting region, or “wall,” the reacting ions may be able to reach the wall very efficiently and escape, even from regions that are many thermal ion mean free paths from the boundary. This process depletes the high-energy ion tail distribution and results in a reduction of the fusion reactivity, causing, ultimately, a substantial reduction in neutron yield in inertial fusion experiments.

This Letter presents an approximate asymptotic theory of the Knudsen layer reduced fusion reactivity. The reactivity $\langle \sigma_{\text{fus}} v \rangle$ is found to be a function of the ion temperature and the Knudsen number $N_K = \lambda_i/L$, where λ_i is the mean free path of the thermal ions and L is the system scale: $\langle \sigma_{\text{fus}} v \rangle \rightarrow \langle \sigma_{\text{fus}} v \rangle(T_i, N_K)$. This is a nonlocal reactivity that depends on the system scale L , typically proportional to the distance to the wall. The effective wall distance can be expressed as a function of location in an inertial confinement fusion (ICF) capsule fuel volume, giving a prescription that can be implemented economically in radiation-hydrodynamic simulations of capsule implosions. The present work builds on a suggestion by Henderson [1] and Petschek and Henderson [2] who first pointed out the possibility of significant tail depletion in idealized deuterium-tritium “microspheres”. The primary contributions of the present work are to develop an asymptotic theory that is simple yet complete enough to allow practical applications, to carry out the model implementation and validation on real present-day implosion experiments, and to demonstrate the power of the model to account for observed results. Over-prediction of fusion yield has been a persistent enigma that has been traditionally corrected by empirical models of “mix”. The

Knudsen layer fusion reactivity reduction outlined here offers a new physical mechanism which may help resolve this enigma.

In ICF settings, nuclear fusion reactions at energies below several hundred keV involve quantum tunneling through the Coulomb barrier. The energy dependence of the fusion cross section $\sigma_{\text{fus}}(E)$ is primarily determined by the Gamow tunneling probability and thus proportional to $\exp(-\sqrt{E_G/E})$, where E is the kinetic energy in the center-of-momentum frame, $E_G = 2\pi^2 Z_1^2 Z_2^2 (e^2/\hbar c)^2 \mu c^2$ is the Gamow energy (1183.3 keV for equimolar DT), and $\mu = m_D m_T / (m_D + m_T)$ is the reduced mass for DT interactions. In the reactivity integral, this rapid increase of the cross section competes with the rapid decrease of the ion distribution function f_i as energy increases. For ions in thermal equilibrium, this distribution would be Maxwellian, $f_i(E)dE = (2/\sqrt{\pi}) T_i^{-3/2} \exp(-E/T_i) E^{1/2} dE$, at the ion temperature T_i , resulting in a reactivity versus energy with a broad maximum at the Gamow peak,

$$\frac{E_0}{T_i} = \left(\frac{E_G}{4T_i} \right)^{1/3} \gg 1. \quad (1)$$

Knudsen layer losses at these energies could have a large effect in decreasing the fusion reactivity.

At distances L of the order of a mean free path λ_i from a wall, hydrodynamics does not hold and a kinetic theory treatment is required. This is the Knudsen layer of the classical kinetic theory of gases, a region of so-called “molecular flow”, where particles directed toward the wall will, on average, reach it following straight line trajectories without undergoing a collision. In a fully ionized DT plasma, the potential for a sizable effect on the fuel ions is enhanced by a Coulomb collision mean free path that scales like energy squared.

We compute the tail distribution from kinetic theory including the Knudsen layer wall losses. To arrive at a tractable theory, we make several approximations.

First, we assume a one-dimensional (1D), planar, spatial geometry and ignore the effects on ion dynamics of ambipolar electric fields or possible thermoelectric magnetic fields. The extension to spherical gas cavities will be given below. Second, we treat the sparse population of tail ion particles as a perturbation, ignoring their effects upon the bulk (Maxwellian) ions. Finally, we regard the ions as a single representative species and assume that tail ions have a speed $v \gg v_{Ti} \equiv (2T_i/m_i)^{1/2}$. In this limit and with these approximations, the ion kinetic equation is of the form

$$\frac{\partial f_i}{\partial t} + v\mu \frac{\partial f_i}{\partial z} = \frac{1}{2} v_{ii}^\mu \frac{v_{Ti}^3}{v^3} \frac{\partial}{\partial \mu} (1 - \mu^2) \frac{\partial f_i}{\partial \mu} + C_{ii}^E(f_i, f_i), \quad (2)$$

where the linear velocity magnitude or energy scattering part of the collision operator for the tail ion population is

$$C_{ii}^E(f_i, f_i) = v_{ii}^E \frac{v_{Ti}^3}{v^2} \frac{\partial}{\partial v} \left(f_i + \frac{T_i}{m_i} \frac{1}{v} \frac{\partial}{\partial v} f_i \right). \quad (3)$$

For high energy DT tail particles, the base collision frequency is given by,

$$\nu_i \equiv \frac{4\pi\rho e^4 \ln\Lambda}{m_i^2 v_{Ti}^3 m_p \langle A \rangle}, \quad (4)$$

where ρ is the mass density, m_p is the proton mass, and $\langle A \rangle$ is the average mass number. The factors which distinguish the pitch-angle and energy scattering frequencies are $\nu_{ii}^\mu = \nu_i \langle Z_b^2 \rangle$ and $\nu_{ii}^E = \nu_i \langle Z_b^2 m_i / m_b \rangle$, where the averages are concentration weighted sums over all the field particle ion components b , and Z_b is the species charge. Here, we denote the cosine of the velocity pitch angle θ relative to \hat{z} by $\mu \equiv \cos\theta$. If v were held fixed in Eq. (2), the kinetic equation would contain only convection and pitch-angle scattering, which together are known to yield spatial diffusion asymptotically over long time and spatial intervals [3,4]. We approximate this behavior in our model by the use of an effective diffusion operator that can be expressed dimensionally as

$$C_K(f_i) \equiv \frac{D}{2} \frac{\partial^2 f_i}{\partial z^2} = \frac{\zeta_0 v^5}{v_{Ti}^3 v_{ii}^\mu} \frac{\partial^2 f_i}{\partial z^2} \rightarrow -v_{ii}^E \zeta_T \frac{2v_{Ti}^2}{v_i^2 L^2} \frac{v^5}{v_{Ti}^5} f_i, \quad (5)$$

and that approximates a diffusive loss of tail ions to a perfectly absorbing wall. Here, we combined all various numerical factors into a single transport coefficient ζ_T of order unity, $\zeta_T \equiv \zeta_0 / (\langle Z_b^2 m_i / m_b \rangle \langle Z_b^2 \rangle)$. The constant, $\zeta_0 \approx 0.33$, may be determined by integrating Eq. (2) with $C_{ii}^E(f_i, f_i) \rightarrow 0$ numerically, by writing the kinetic equation as an equivalent set of Itô stochastic differential equations and integrating numerically. Note that it is the pitch-angle scattering that determines the spatial diffusion rate and that this scattering is greater than energy scattering with the addition of high Z species. Although the approximate

nature of the model suggests that the constant ζ_0 can be regarded as a parameter to be calibrated empirically, we have not done so in this Letter, but rather have kept with the value $\zeta_0 = 0.33$.

Diffusion overestimates losses somewhat very near the wall. Indeed, this operator becomes singular as $L \rightarrow 0$, an indication that a more complete treatment of the transport is needed. For the purpose of this initial study, however, it is efficient to err on the side of overestimating the effect, because then, if no observable consequences are seen in the numerical simulations, we may be confident that the ion-loss effect is negligible. We do find observable consequences, however, as described below, which thus motivate more accurate transport solutions, which are now in progress.

Rewriting Eq. (2) in terms of the dimensionless energy variable $\varepsilon \equiv m_i v^2 / 2T_i$ gives the equation for the steady state tail ion distribution function

$$0 = \frac{\partial}{\partial \varepsilon} \left[f_i + \frac{\partial}{\partial \varepsilon} f_i \right] - N_K^2 \varepsilon^3 f_i. \quad (6)$$

In this expression the Knudsen number, the ratio of mean free path to scale length for the thermal particles, is given by

$$N_K = \frac{\lambda_i}{L} = \sqrt{\zeta_T} \frac{T_i^2 \langle A \rangle m_p}{\pi \rho e^4 \ln\Lambda L} \approx 0.092 \frac{\langle A \rangle}{2.5} \frac{4}{\ln\Lambda} \frac{T_i^2}{\rho L}, \quad (7)$$

with T_i in keV and L in μm , for singly charged particles. The factor ζ_T has been absorbed into the definition of the Knudsen number, combining the two processes of pitch-angle and energy scattering.

For simplicity, at first, we take all ions to be identical particles with mass $A = 2.5$, as for equimolar DT. We will use the Spitzer expression for $\log\Lambda$ in the applications to follow. For $N_K \ll 1$ and neglecting the Knudsen loss term in Eq. (6), one gets the Maxwellian distribution, $f_i \sim \exp(-\varepsilon)$, as expected. The balance that produces the Maxwellian in Eq. (6) is between frictional drag, the first term, and energy diffusion to higher energy, the second term. When the Knudsen loss is taken into account, the tail is depleted and the energy flow to higher energies increases to balance this loss to the wall. The overall ion particle number density is assumed to be maintained by a return flow, spatially, at lower energies outside the domain of this calculation. This is identical to the process that occurs microscopically in ion thermal conduction, a process that also results in tail depletion.

Equation (6) for $\varepsilon^3 N_K^2 \gg 1$ can be approximated using the WKB method and matched to the Maxwellian at low energies to give the *Knudsen distribution function*,

$$f_K \approx \frac{2}{\sqrt{\pi + N_K \varepsilon^{3/2}}} \exp\left(-\varepsilon - \frac{2}{5} N_K \varepsilon^{5/2}\right). \quad (8)$$

Equation (8) is a simplified version of a more accurate Padé approximant, used here for its physical clarity and to avoid

underestimating the ion-loss effect, in the spirit of efficiency mentioned earlier. The strong energy dependence of the Knudsen factor in the exponent makes tail depletion significant. For example, for a Knudsen number $N_K = 0.1$ at the ion temperature $T_i = 5$ keV and a tail population at energy 20 keV (the energy of the Gamow peak), the reactivity is reduced by a factor of 4 compared with that of a Maxwellian.

Modifications to fusion reactivities can be estimated from this Knudsen distribution function by use of the Bosch-Hale formula for the DT cross section [5]; this formula is based on a Padé approximant fit to the data after extracting the Gamow factor and is accurate to 2% in the center-of-mass energy range from 0.5 to 500 keV. The integral was carried out to produce a reactivity table, $\langle\sigma_{\text{fus}}v\rangle(T_i, N_K)$, as a function of two variables: the ion temperature and the Knudsen number. It is a *nonlocal* reactivity which depends on the distance to the absorbing wall, as well as the ion temperature and fuel density. Figure 1 shows the reactivity reduction ratio, defined as $\langle\sigma_{\text{fus}}v\rangle(T_i, N_K)/\langle\sigma_{\text{fus}}v\rangle(T_i, 0)$, as a function of temperature at various Knudsen numbers. This figure allows simple estimates of the expected amount of yield reduction in various situations. For a typical hot OMEGA [6] implosion as discussed below, with $T_i \approx 9$ keV, $\rho \approx 6$ g/cm³, $L \approx 10$ μ m, $\langle A \rangle = 2.5$, and $\ln \Lambda \approx 6$, Eq. (7) implies $N_K \approx 0.083$. From Fig. 1, we expect a yield reduction by about a factor of 4.

The theory described above is appropriate for a 1D planar wall. For ICF capsules in an idealized 1D spherical geometry, Knudsen-layer ions are lost to the full 4π solid angle. In this case we calculate the effective length as appropriate for the diffusion losses from a reciprocal root-mean square, normalized such that for the single planar wall case the result is simply the distance to the wall. This average goes to the two limits $L_{\text{eff}} \rightarrow R_0/\sqrt{6}$ as $r \rightarrow 0$ and $L_{\text{eff}} \rightarrow (R_0 - r)$ as $r \rightarrow R_0$.

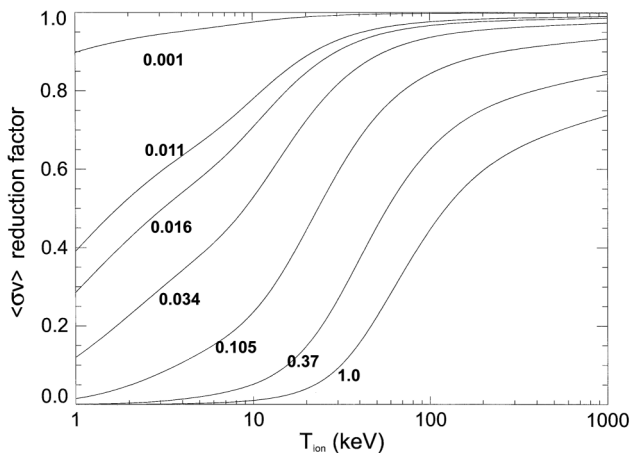


FIG. 1. Reduction ratio vs T_{ion} for values of N_K as shown.

The theory for Knudsen layer losses of tail ions has been implemented in a radiation-hydrodynamics code and used to perform simulations of implosions of DT-filled ICF capsules. The purpose of the computational study is to demonstrate that (a) the Knudsen-reactivity model has a significant effect in simulations of ICF capsules and (b) the effect is in the right direction for explaining and predicting experiments. It is not justifiable, however, to claim that the study conclusively proves the presence or absence of a particular physical phenomenon in capsule implosions, owing to the integral and approximate nature of multi-physics simulation codes.

The simulations assume a 1D spherically symmetric geometry. At each time step in the simulation, the Knudsen-reactivity model calculates the Knudsen number in each computational cell of the DT fuel as a function of the cell's ion temperature, composition, mass density, radial location r , and the radius R_0 of the inner edge of the ablator, as given by Eq. (7). The Coulomb logarithm is calculated using Spitzer's expression including quantum corrections [7]. The effective length L_{eff} is evaluated numerically, separately from the radiation-hydrodynamics simulation and used to evaluate L_{eff} in each cell of the DT fuel. Given N_K and T_i in each cell, a bilinear interpolation is performed in the table of reactivity reduction ratios to find the reduction ratio appropriate for the cell. Then the nominal reactivity for the cell used by the code is multiplied by the reduction ratio.

We have carried out simulations of a variety of plastic-shell capsule implosion shots conducted at OMEGA [6] during 2005–2011. The implosions were selected to be highly diverse, spanning $2\frac{1}{2}$ orders of magnitude in observed yield and a factor of 4 in the observed ion temperature. The fuel gas molar composition ranged from $T:D = 0.55:1$ to $T:D = 585:1$, more than 3 orders of magnitude. Several of the capsules were the deuterated-shell implosions and corresponding “reference” implosions analyzed by Wilson *et al.* [8]; these capsules give unambiguous evidence for ion-species mixing at the scale of an ion mean free path (“atomic mix”). All capsules were driven symmetrically by 60 beams of the OMEGA laser.

The simulations used as-shot capsule dimensions, fuel fill pressure and composition, and laser pulse energy. A typical SG1018 1-ns square pulse shape (as used on OMEGA shot 55995) was assumed for all simulations, scaled to deliver the appropriate energy for each shot. The simulations incorporated multigroup radiation diffusion, charged-fusion-product diffusion, flux-limited electron thermal diffusion, and laser energy propagation via geometric ray tracing and deposition by inverse bremsstrahlung. Turbulent mixing was accounted for using the buoyancy-drag model of Dimonte [9] with drag coefficient 2.5 and an initial scale length $l = 0.2$ μ m. Because mixing replaces the sharp boundary of the capsule shell with a gradient in composition, the “wall” was identified as

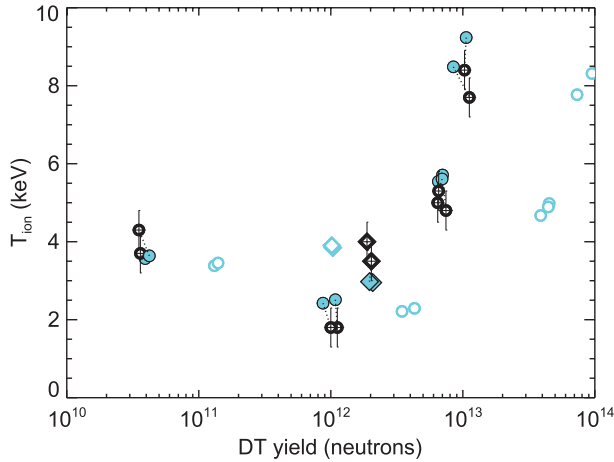


FIG. 2 (color). Comparison of observed (black symbols) and simulated (blue symbols) DT neutron yields and ion temperatures for the OMEGA capsules discussed in the text. Open blue symbols show “nominal” simulations. Filled blue symbols show simulations using the Knudsen + mix model. Circles indicate ordinary plastic-shell capsules. Diamonds show deuterated-shell capsules. The Knudsen + mix model gives markedly improved agreement with observations, compared to nominal.

the radial location at which the fusion rate drops to 0.001 of its peak value. Radiative opacities were computed using a non-LTE model. The electron thermal flux limiter was set equal to 0.06 [10,11]. To account for laser refraction past the capsule (since the laser beam illumination geometry cannot be correctly represented in one dimension) and nonlinear scattering processes (which are not modeled at all in the code), the incident laser energy was modified to find the best agreement between the calculated and observed yield, ion temperature, and bang time for each capsule, as is typically done for such simulations [12].

Figure 2 is a plot showing the results of each OMEGA shot as a black symbol with error bars, whose horizontal coordinate is the observed DT neutron yield Y_{obs} , and whose vertical coordinate is the observed burn-rate-weighted average ion temperature $T_{\text{ion,obs}}$. Two radiation-hydrodynamics simulations (at least) were performed for each shot, one of which (the “nominal” simulation) did not invoke either the Knudsen-layer reactivity model or the Dimonte buoyancy-drag mix model, while the other (the “Knudsen + mix model” simulation) invoked both. Figure 2 shows the nominal simulations as open symbols, and the Knudsen + mix model simulations as filled blue symbols joined by a dashed line to the corresponding observed point. The Knudsen + mix model is clearly in significantly better agreement with the observations than is the nominal model. As a measure of the improvement, we compute the quantity D^2 , the average over all shots of the squared distance between the observed and simulated points in Fig. 2, measured in units of the error bars $\sigma_{\log Y} = \log_{10}(1.10) \approx 0.041$, corresponding to 10% uncertainty in yield, and $\sigma_T = 0.5$ keV. We can compute D^2 separately

for the nominal simulations and the Knudsen + mix model simulations, with the result that $D_{\text{nom}} = 16.3$ while $D_{\text{Knud+mix}} = 1.9$. In this metric, the Knudsen + mix model thus provides a better representation of the observations by a factor of 8.6.

In these simulations, the Knudsen-reactivity model usually has a stronger effect on yield than does the mix model. For example, for a typical implosion with an ~ 8 keV ion temperature, the Knudsen-reactivity model alone reduces the yield by a factor of 5.4 from its nominal value, while the mix model alone reduces the yield by a factor of only 2.1. In deuterated capsules, on the other hand, the mix model has a stronger effect than the Knudsen-reactivity model, because the denominator $\langle Z_b^2 m_i / m_b \rangle \langle Z_b^2 \rangle$ in the expression for ζ_T becomes large in a mixture of C, D, and T, reducing the ion mean free path.

A comparison of the relative merits of the mix models with different scale lengths l , or of the mix models alone, ignoring the Knudsen-reactivity model, will await a future study with global optimization and rigorous hypothesis testing, beyond the scope of the present work. But we can already say that it is likely that a Knudsen + mix model of the kind described here will have superior explanatory power compared to a mix model alone. Considering just a typical 8-keV implosion and a typical 2-keV implosion from Fig. 2, using only the mix model but omitting the Knudsen-reactivity model, we can search for a best-fit l for these two implosions that minimizes D^2 averaged over the two shots. The resulting $D^2(l)$ has a minimum at $l \approx 0.4 \mu\text{m}$ with a value of $D = 3.2$, more than 50% larger than the value of $D_{\text{Knud+mix}}$ found above for all eleven shots of Fig. 2. This result is preliminary evidence that the mix model alone will have difficulty accounting for all shots with a single value of l as readily as the Knudsen + mix model can.

Initial applications of this model to the cryogenic NIF ignition capsule show negligible effect on the occurrence of ignition in 1D spherically symmetric simulations. The low temperature and high density of the fuel at ignition, and the continuously increasing temperature and density gradients throughout the hot spot and cold fuel, combine to reduce the effect of Knudsen-layer ion loss. Its effect in two-dimensional or three-dimensional simulations remains for future investigation.

Large anomalies in the fusion reaction ratios (for DD reactions and TT reactions relative to the dominant DT reactions) have been observed [13] on OMEGA and attributed to baro-diffusion induced fuel stratification [14]. All the qualitative features of the observed anomaly (that the observed yield ratios Y_{dd}/Y_{dt} were low relative to calculations while the ratios Y_{tt}/Y_{dt} were high, that the anomaly increased with temperature, and that the effect was larger for the TT/DT anomaly) are intrinsic features of the Knudsen reactivity reductions described in this

Letter. More definitive and quantitative statements await a detailed analysis.

The authors thank Marv Alme, Charlie Snell, Michael Steinkamp, Joann Campbell, and George B. Zimmerman for numerous discussions over the past year in developing the model. We also thank Jim Cobble, Vladimir Glebov, Doug Wilson, and Yongho Kim for providing observed data and gas-fill information for the capsules discussed here, and Evan Dodd for advice on calibrating the radiation-hydrodynamic simulations. We are most grateful to a reviewer for suggesting we combine the Knudsen phenomenon with mix. Work performed under the auspices of the U.S. Department of Energy by the Los Alamos National Security, LLC, Los Alamos National Laboratory.

[1] Dale B. Henderson, *Phys. Rev. Lett.* **33**, 1142 (1974).

[2] A.G. Petschek and D.B. Henderson, *Nucl. Fusion* **19**, 1678 (1979).

[3] H.A. Bethe, M.E. Rose, and L.P. Smith, *Proc. Am. Philos. Soc.* **78**, 573 (1938).

[4] B.J. Albright, B.D.G. Chandran, S.C. Cowley, and M. Loh, *Phys. Plasmas* **8**, 777 (2001).

[5] H. S. Bosch and G. M. Hale, *Nucl. Fusion* **32**, 611 (1992).

[6] T.R. Boehly *et al.*, *Opt. Commun.* **133**, 495 (1997).

[7] L. Spitzer, Jr. *Physics of Fully Ionized Gases* (Interscience, New York 1962), Eqs. (5)–(14).

[8] D.C. Wilson, P.S. Ebey, T.C. Sangster, W.T. Shmayda, V. Yu. Glebov, and R.A. Lerche, *Phys. Plasmas* **18**, 112707 (2011).

[9] G. Dimonte, *Phys. Plasmas* **7**, 2255 (2000).

[10] R.L. Morse and C.W. Nielson, *Phys. Fluids* **16**, 909 (1973).

[11] R.C. Malone, R.L. McCrory, and R.L. Morse, *Phys. Rev. Lett.* **34**, 721 (1975).

[12] E.S. Dodd, J.F. Benage, G.A. Kyrala, D.C. Wilson, F.J. Wysocki, W. Seka, V. Yu. Glebov, C. Stoeckl, and J.A. Frenje, *Phys. Plasmas* **19**, 042703 (2012).

[13] D.T. Casey *et al.*, *Phys. Rev. Lett.* **108**, 075002 (2012).

[14] P. Amendt *et al.*, *Phys. Rev. Lett.* **105**, 115005 (2010).